Heating Studies Without 3HC

Fernando H. de Sá, Gustavo R. Gomes, Iago C. de Almeida,
Walter Marchesini Jr., Liu Lin, Ximenes Resende,
Murilo B. Alves

May 16, 2024

1 Introduction

SIRIUS RF power plant upgrade will be ready for commissioning by mid 2024. Once this system is operating, it will allow increasing the stored current in users operations to 350 mA with the design nominal voltage of 3 MV, considering the energy loss by dipoles and all the undulators of Phase I of operation. The expected natural bunch length at this voltage is approximately 2.4 mm. This small bunch imposes a large wake-field induced heat-load on the accelerators components and shorten the Touschek Lifetime of the machine. During design stage a third-harmonic cavity (3HC) was considered to lengthen the bunches and alleviate these effects. However, the installation of this cavity is not planned for the near future. This work describes an study to estimate the maximum stored current SIRIUS storage ring can operate without the 3HC, while keeping a reasonable lifetime for top-up operation and no heating issues.

To estimate the heating load for higher currents we combined experiments in the machine with different filling patterns with estimates from the impedance budget model. Most of the heating load of SIRIUS storage ring is due to broad-band impedances, according to the model. For this type of wake-field the heat-load depends on the squared sum of the filling pattern and on the total current squared. This means that we can estimate the heating load of a filling pattern with smaller squared sum and higher total current using another filling with higher squared sum and smaller total current. This method is useful for SIRIUS because the current total power available by the RF system limits the maximum stored current to 100 mA, with a gap voltage of ∼1.57 MV. SIRIUS operates with uniform filling, which is the filling pattern with the smallest possible squared sum. This way, by using any other filling pattern at 100 mA, we can estimate the heating load of the uniform filling at higher currents.

Another way of estimating the heat-load for future operations consists in decreasing the gap voltage of the cavity. With smaller voltage, the power consumption of the cavity itself decrease, which allows increasing the total stored current. Currently, SIRIUS operates with a PETRA 7-Cell cavity at a gap voltage of ∼1.57 MV and its power plant has ∼100 kW of available power. From this, ~50 kW is used to keep the gap voltage and the remaining power is consumed by the 100 mA beam. Estimates show that decreasing the gap voltage to ~0.7 MV would still keep Touschek lifetime above 1 h (the energy loss per turn in SIRIUS storage ring is ~480 keV) and allow the maximum stored current to increase to ~170 mA. This method has the advantage of keeping the same filling pattern of regular operation, thus sampling the impedance at the same harmonics, which also serves as an estimate of the effect of narrow band impedance sources. On the other hand, the bunch length is larger at lower gap voltages, which limits the impedance range sampled by the beam and underestimate the broadband effect. The natural bunch length at current nominal operations is ~3.2 mm and with 0.7 MV of gap voltage it would increase to 5.8 mm and reduce the frequency bandwidth of the beam from ~30 GHz to ~17 GHz. Simulations with the impedance budget shows that the current increase is not sufficient to compensate the larger bunch length for most components, such that the resulting power load is smaller in this configurations. Among the few components the larger current does increase the power load is the direct-current current transformer (DCCT) and the longitudinal kicker for the bunch-by-bunch (BbB) feedback system. Another possible practical disadvantage of this method of estimating the power load at higher currents is related to coupled-bunch instabilities. The lower cavity voltage reduces the synchrotron tune, which decreases the longitudinal instability threshold. For SIRIUS this might be a problem because at 100 mA and nominal gap voltage the beam is already unstable due to higher-order modes (HOMs) of the PETRA 7-Cell cavity and is stabilized by the BbB. With the lower tune, the instability would be stronger and the BbB would probably not be able to control the instability anymore.

2 Theory of Heating Load

The Power deposited by the beam in a component of the vacuum chamber is given by

$$P = I_\mathrm{t}^2 T_0 \frac{\omega_0}{2\pi} \sum_{p=-\infty}^{\infty} \left|\tilde{\lambda}(p\omega_0)\right|^2 \mathrm{Re}\left\{Z(p\omega_0)\right\} \tag{1}$$

where $I_\mathrm{t} > 0$ is the total current of the beam, T_0 and ω_0 are the revolution period and angular frequency of the storage ring, Z is the longitudinal impedance of the component and

$$\tilde{\lambda}(\omega) = \int_{-\infty}^{\infty} \mathrm{d}z \lambda(z) e^{i\omega z/c}, \tag{2}$$

where c is the speed of light and $\lambda(z)$ is the longitudinal distribution of the beam, which can be written as

$$\lambda(z) = \sum_{\ell=0}^{h-1} F_\ell \lambda_\ell(z - \ell\lambda_\mathrm{rf}), \tag{3}$$

where h is the harmonic number of the ring, $\lambda_{\mathrm{rf}} = cT_0/h$ is the rf wavelength, $\lambda_\ell(z)$ is the distribution of the ℓ-th bunch and $F_\ell \geq 0$ are the components of the filling pattern vector,

$$F = \left(\frac{I_0}{I_{\mathrm{t}}}, \ldots, \frac{I_{h-1}}{I_{\mathrm{t}}}\right)^{\mathrm{T}} \quad \text{with} \quad F_\ell = \frac{I_\ell}{I_{\mathrm{t}}}, \tag{4}$$

which sums to unity. Since the bunch distributions are normalized to unity, then the beam distribution is also normalized to unity.

The Fourier transform of the longitudinal distribution is then given by

$$\tilde{\lambda}(\omega) = \sum_{\ell=0}^{h-1} F_\ell \tilde{\lambda_\ell}(\omega) e^{i\ell\omega\lambda_{\mathrm{rf}}/c} \tag{5}$$

and its squared modulus is

$$\left|\tilde{\lambda}(\omega)\right|^2 = \tilde{\lambda}(\omega)\tilde{\lambda}^*(\omega) = \sum_{\ell=0}^{h-1} F_\ell \tilde{\lambda_\ell}(\omega) e^{i\ell\omega\lambda_{\mathrm{rf}}/c} \sum_{k=0}^{h-1} F_k \tilde{\lambda_k}^*(\omega) e^{-ik\omega\lambda_{\mathrm{rf}}/c}. \tag{6}$$

Defining the quantity

$$B(\omega) = \sum_{\ell=0}^{h-1} F_\ell e^{i\ell\omega\lambda_{\mathrm{rf}}/c} \tag{7}$$

and assuming all bunches are equally distributed

$$\lambda_k(z) = \lambda_0(z), \quad \forall k \in [0, h-1], \tag{8}$$

then the modulus squared of the distribution is simplified to

$$\left|\tilde{\lambda}(\omega)\right|^2 = \left|\tilde{\lambda_0}(\omega)\right|^2 |B(\omega)|^2. \tag{9}$$

Inserting equation above on the power loss expression, we get

$$P = I_{\mathrm{t}}^2 T_0 \frac{\omega_0}{2\pi} \sum_{p=-\infty}^{\infty} \left|\tilde{\lambda_0}(p\omega_0)\right|^2 |B(p\omega_0)|^2 \operatorname{Re}\{Z(p\omega_0)\}. \tag{10}$$

Note that

$$B(p\omega_0) = \sum_{\ell=0}^{h-1} F_\ell e^{i2\pi p\ell} = \mathrm{DFT}(F)_p^*, \tag{11}$$

where $\mathrm{DFT}(F)_p^*$ denotes the complex conjugate of the p-th component of the discrete Fourier transform (DFT) of the filling pattern vector.

Since the filling pattern has length h, its DFT has the following property

$$B((p+h)\omega_0) = B(p\omega_0), \tag{12}$$

which allows us to write the power loss in the following convenient form

$$P = I_{\mathrm{t}}^2 T_0 \frac{\omega_0}{2\pi} \sum_{\ell=0}^{h-1} |B(\ell\omega_0)|^2 \sum_{p=-\infty}^{\infty} \left|\tilde{\lambda_0}((ph+\ell)\omega_0)\right|^2 \mathrm{Re}\left\{Z((ph+\ell)\omega_0)\right\}. \quad (13)$$

Now, if we assume the impedance varies slowly in the frequency scale of the rf frequency, i.e., it is a broad band impedance,

$$Z((ph+\ell)\omega_0) \approx Z(ph\omega_0), \quad \forall\, p \in \mathbb{Z} \text{ and } \ell \in [0, h-1], \quad (14)$$

and remembering the Parseval's theorem for the DFT [1]

$$\sum_{\ell=0}^{h-1} |B(\ell\omega_0)|^2 = h \sum_{\ell=0}^{h-1} F_\ell^2 = h|F|^2, \quad (15)$$

we can write the power loss as

$$P \approx I_{\mathrm{t}}^2 \, |F|^2 \, T_0 \frac{h\omega_0}{2\pi} \sum_{p=-\infty}^{\infty} \left|\tilde{\lambda_0}(ph\omega_0)\right|^2 \mathrm{Re}\left\{Z(ph\omega_0)\right\}, \quad (16)$$

where we note it depends on the square of the total current stored and on the modulus squared of the filling pattern vector. Defining the loss factor

$$\kappa = \frac{h\omega_0}{2\pi} \sum_{p=-\infty}^{\infty} \left|\tilde{\lambda_0}(ph\omega_0)\right|^2 \mathrm{Re}\left\{Z(ph\omega_0)\right\} \approx \frac{1}{2\pi} \int_{-\infty}^{\infty} \mathrm{d}\omega \left|\tilde{\lambda_0}(\omega)\right|^2 \mathrm{Re}\left\{Z(\omega)\right\}, \quad (17)$$

the power loss can be summarized as

$$P \approx I_{\mathrm{t}}^2 \, |F|^2 \, T_0 \, \kappa. \quad (18)$$

The modulus squared of the filling pattern is minimum for uniform filling, $|F|^2 = 1/h$, and maximum for a single-bunch, $|F|^2 = 1$. Also, for simplified filling patterns with M arbitrarily spaced bunches with the same current per bunch, we have $|F|^2 = 1/M$.

3 Model Calculations

Figure 1 shows the power loss predicted by the impedance budget model of the SIRIUS storage ring for each component of the vacuum chamber when the gap voltage of the cavity is varied and uniform filling is considered. Note the strong dependence of the power loss with the bunch length. Figure 2 shows the model prediction for power loss for different filling patterns. Since most of the components are dominated by broad band impedances, the power loss do not depend too much on the filling pattern.

From these results we see that the taper transition of the superconducting rf cavities is the single component with the larger power loss reaching approximately 500 W at 200 mA in uniform filling and 3 MV in the rf cavities. The second class of components with large power deposition are the striplines, ranging from 30 W to 90 W of deposited power.

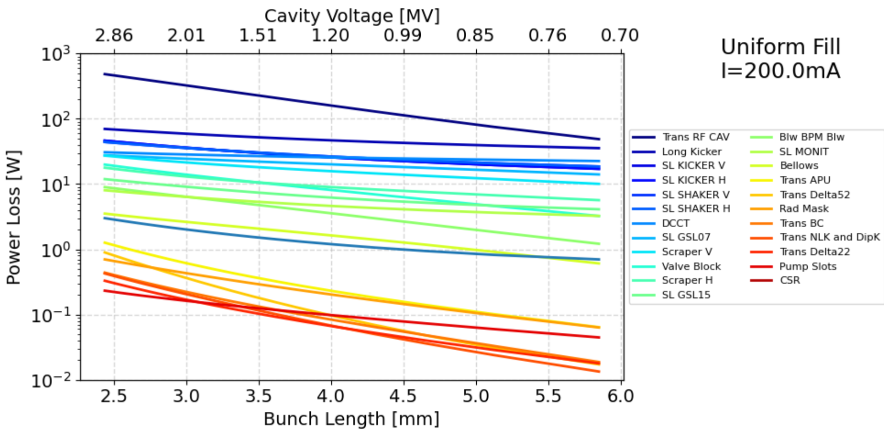

Figure 1: Power loss for each component of the impedance budget model as function of the cavity voltage and bunch length.

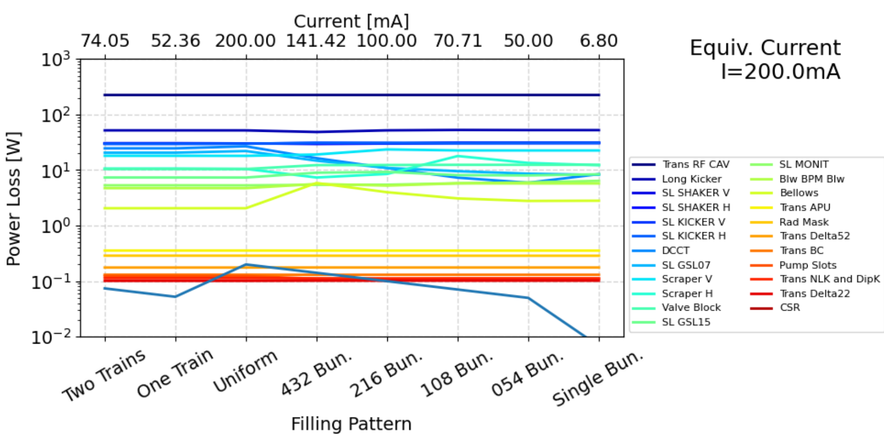

Figure 2: Power loss for each component of the impedance budget model for several filling patterns. The total current used for each filling pattern was calculated using (18) so that the equivalent current in uniform filling was kept constant and equal to 200 mA. The nomenclature "N Bun." refers to fillings with N equally spaced bunches.

4 First Machine Shift (2023/07/25)

Several temperature and pressure PVs were monitored during this study via archiver viewer. Table 1 has links to these PVs in the time interval of the experiment.

- Before the machine study there was 100 mA stored in the ring with nominal operation conditions;
- From this point, we tried to decrease the gap voltage of the cavity and increase the current so that the total power consumption of the cavity stayed constant;
- It was difficult to keep the beam stable in the longitudinal plane, so the process was slow;
- When we were at 107.5 mA there was a beam dump of an so far unknown cause;
- We tried again, but another beam dump happened when we were at 110 mA;
- Another beam dump, now at a current lower than 100 mA;
- Francisco Gabriel, found out the cause for the beam dumps was the temperature of a mirror in the CEDRO beamline. We couldn't identify this earlier because this interlock was not properly mapped in the logging system;
- There was an access to the tunnel to solve a problem with the mirror movement system. In this intervention, they also found a problem with a valve that controls the water flow of the mirror's cooling system;
- Lunch;

4.1 Non-uniform Filing

- After lunch we decided to change plans and study the heating under non-uniform fillings;
- We started by injecting a multi-bunch train of the EGun on the storage ring without changing the bucket list, such that all stored current is located on a single train. The bucket list index used was the bucket 260.
- In our first try the beam was dumped due to a problem in the IMBUIA beamline. There was another access to the tunnel to solve a problem related to the mirrors. We believe these problems with CEDRO and IMBUIA were not related to our study;
- We estimated the bunch profile using the horizontal and vertical BbB and the filling patter oscilloscope. Figure 3 shows the estimated filling pattern;

Location	Description	Link
	Pressures	
Straights	Center of the Straight	link
C1	after B1A	link
C3	after BC	link
	DCCTs Temperatures	
DCCTs	Sectors 13 and 14	link
	Bellows Temperatures	
SA, SB, SP	Straight after valve	link
M2-BG	after gate valve	link
C1-MD	arco C1 pos BPM	link
C1-ED	after BPM close to B2A entrance	link
C2-ED	after BPM close to BC entrance	link
C3-MD1	after BPM at center of C3	link
C4-MD	after BPM at center of C4	link
IDs	IDs	link
	Temperatures by Sector	
01	center of straight and arc	link
02	center of straight and arc	link
03	center of straight and arc	link
04	center of straight and arc	link
05	center of straight and arc	link
06	center of straight and arc	link
07	center of straight and arc	link
08	center of straight and arc	link
09	center of straight and arc	link
10	center of straight and arc	link
11	center of straight and arc	link
12	center of straight and arc	link
13	center of straight and arc	link
14	center of straight and arc	link
15	center of straight and arc	link
16	center of straight and arc	link
17	center of straight and arc	link
18	center of straight and arc	link
19	center of straight and arc	link
20	center of straight and arc	link

Table 1: Links of the temperatures and pressures monitored during the machine study.

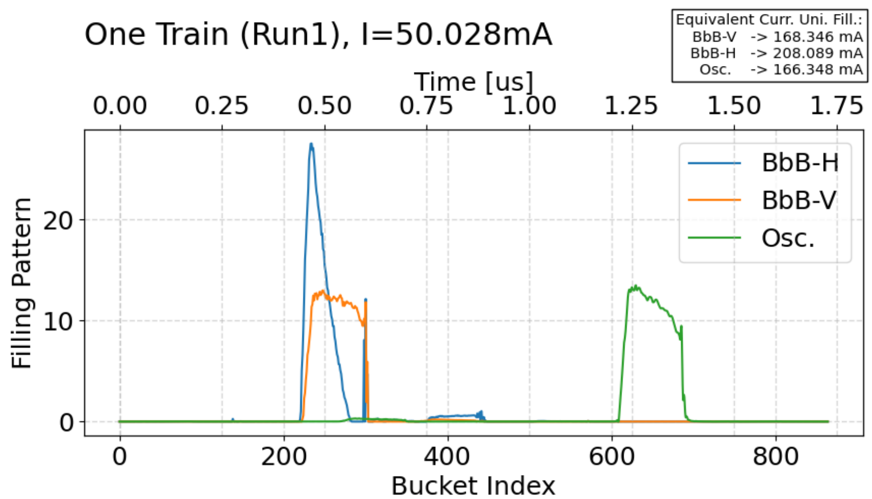

Figure 3: Filling pattern estimation by three different systems. Note the horizontal BbB gives a different filling, probably due to some non-optimal timing configuration. The text shows the equivalent current calculated using each filling.

- In the first try we reached 55 mA and the beam was dumped due to interlock of the vacuum pump of sector 14M1. The valves from sector 13M2 and 14M1 were also closed;
- This same problem also happened for three more runs with the same filling pattern, now at smaller currents: 30 mA, 45 mA and 39 mA. We believe these problems are related to some narrow band impedance of the flange of the DCCT installed in sector 13C4. Such hypothesis is justified by the non-repeatability of the current at which these events happen and on the speed in which they occur. Analysing of the vacuum from that sector via archiver viewer, we noted several sudden pressure peaks, which is in contrast to the slow temperature and pressure rise of other sectors as seen in the graphs of Table 1;
- To try to continue pushing up the estimated current for uniform filling without having these beam dumps, we injected a different filling pattern, with two trains. This filling pattern has a smaller number and intensity of revolution harmonics, and we hoped it would require a higher total stored current to dump the beam;
- With this filling pattern we reached 90 mA of stored current, which amounts to 220 mA in uniform fill in terms of broadband impedance induced heating. Figure 4 shows the estimated filling pattern and the currents in uniform filling.

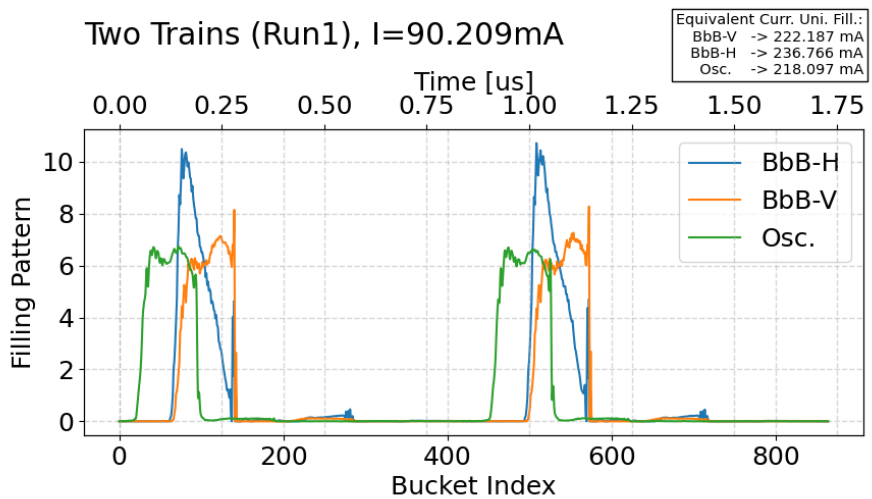

Figure 4: Filling pattern estimation by three different systems. Note the horizontal BbB gives a different filling, probably due to some non-optimal timing configuration. The text shows the equivalent current calculated using each filling.

- At this current the beam was dumped again due to the same interlock as before, when we were injecting in a single train. This sudden dump also corroborates with the hypothesis that relates it with narrow band impedances, because we reached currents whose equivalent uniform fill current are much larger than the ones we reached with the single train;

4.2 Uniform Filling

- After this study we went back to trying to inject currents larger than 100 mA in uniform filling with a lower voltage gap. This time we didn't care for the longitudinal stability, so the beam was always unstable;
- We started with a low gap voltage of ≈1 MV and ramped up the current from zero. At 64 mA the instability of the beam started to compromise the low level rf control and we had to increase the voltage;
- We followed this strategy along the rest of the experiment. We reached 150 mA with a gap voltage of 1.5 MV and using 120 kW of power;
- This graphic shows some variables related to the study described above.

4.3 Final Remarks

This first study indicates that the heating caused by the broad band impedance of the storage ring will not be an issue for operation with currents up to 200 mA.

We will perform more studies to confirm this assumption. In particular, we must make sure the beam dumps of this study were in fact being caused by narrow band impedances and fix the source of this contribution. We also need to let the beam stored for longer periods under the more demanding condition of filling pattern and total current so that the temperatures stabilize.

5 Second Machine Shift (2023/08/01)

In this second machine study we only pursued the idea related to more demanding filling patterns. We did not tried to increase the current beyond 100 mA. Prior to this study, we accessed the tunnel and tightened the screws of the flange of the DCCT from sector 13C4. The screws allowed a modest tightening of approximately 1/3 of turns.

At around 8:00h the archiver crashed and the control netword became unstable. An intervention and restart of archiver was needed. All PVs took too long to connect to archiver, and the system only re-established all connections after lunch (around 13:00h). For this reason the first current ramp made in the morning is not archived. In this run, we reached 65 mA with a single train in the machine. When we were ramping up to 70 mA there was a beam dump to overheating of the vacuum window between the cavity and the waveguide. This interlock setpoint is 100 °C and could not be relaxed during the experiment. This temperature is highly influenced by the stability of the beam. Coupled-bunch oscillations generate extra power deposition on the region of the window. As an example, at nominal operation of 100 mA at uniform filling with stable beam, the temperature only reaches ≈52 °C.

During this first experiment we also fixed the timing configuration of the horizontal BbB so that its filling pattern estimate was in good agreement with the one from the vertical BbB and the oscilloscope. We had to change the phase of the front-end to accomplish this improvement in amplitude detection.

We went to lunch to wait for the Archiver to connect with all relevant PVs, including the one from the window. After lunch we inject a small current (35 mA) in uniform filling to find the right phase for the horizontal BbB feedback coefficients. After that we went back to the single train filling. This time we also reached 65 mA but did not go any further because of the temperature of the window. The graph shows the temperature of the window and the stored current during this experiment. Figure 5 shows the equivalent current reached in this situation. We kept the beam with this current in top-up mode for some time to analyse the evolution of the pressure and temperature of the components. We didn't notice any problems related to the pressure, but some measurements of temperature from sector 1 increased significantly and did not stabilize during the whole experiment, reaching ≈53 °C before we dumped the beam. We don't know yet to which component this measurement refers, but we will access the tunnel next Monday morning (2023/08/06) to map the sensor position. Most probably though, it refers to the vertical scraper.

Next, we injected the beam in two trains. In this configuration we could

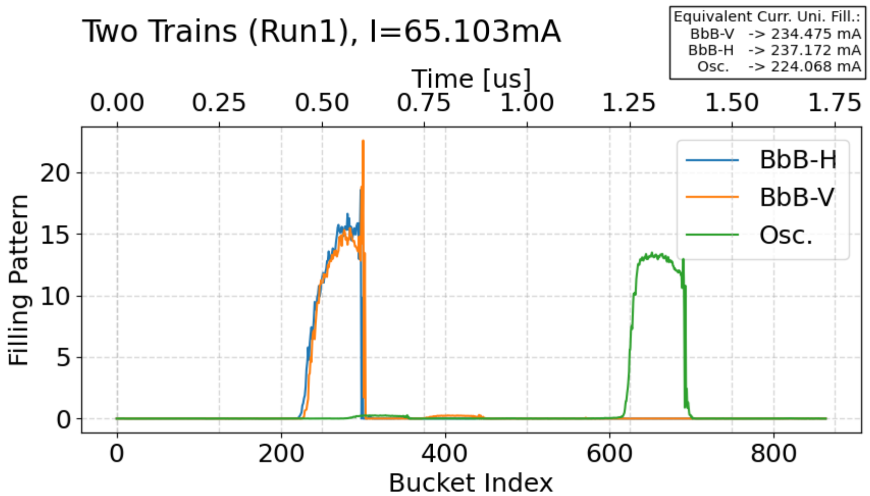

Figure 5: Filling pattern estimation by three different systems. The text shows the equivalent current calculated using each filling.

reach 90 mA and the temperature of the window was kept at 96 °C. The same heating problem was observed in sector 1. Figure 6 shows the equivalent current of this filling. The similarity to the single train estimated current together with the same heating behavior, corroborates with the hypothesis of broadband induced power on the component close to the sensor.

We ended the machine shift at around 17:00h to start recovering the machine for users operation.

6 Third Machine Shift (2024/05/13)

- We started the experiment at 18h. There was 4.3 mA stored in the machine localized in a single train;
- We disabled the orbit interlock and adjusted the BPMs attenuation to 31;
- We reconfigured the sum threshold value of the orbit interlock: we acquired the signal from BPMs using the window and multiplied the value by 2.33 so that the signal were equivalent to a 10 mA beam;
- We enabled back the orbit interlock;
- We tested changing the LLRF parameters in flight to check whether the system would interlock. First we lowered the proportional to 3 and then the integral to 30. The system didn't interlock. We went back to the original values of 8000 for the integral and 155 for the proportional, starting with the integral;

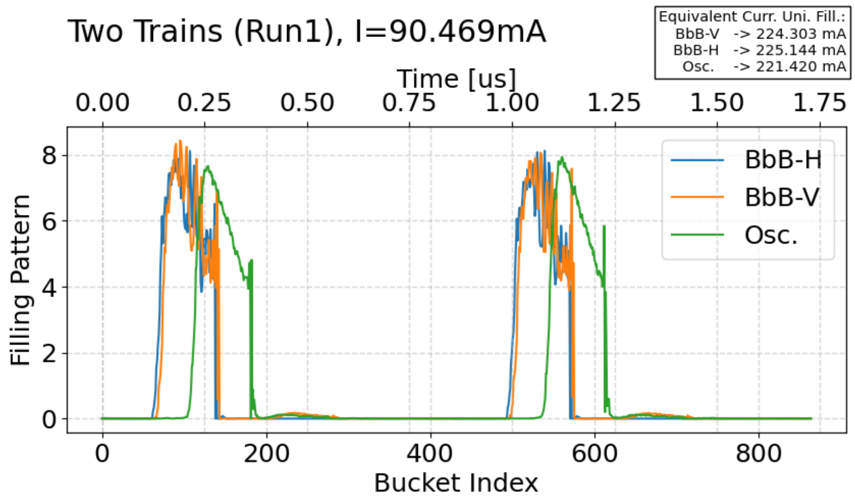

Figure 6: Filling pattern estimation by three different systems. The text shows the equivalent current calculated using each filling.

- We dumped the beam and injected two trains centered in buckets 260 and 692, diametrically opposed to each other;
- We were able to inject 90 mA in total. The temperature of sensor MD4 of sector 1 risen again and stabilized at 49 °C, almost in accordance with previous experiments. Check the graph;
- We left the beam in top-up mode for more half hour and then lowered the current to 80 mA. We left the beam in this condition for more time and the temperature droped to 47 °C;
- We killed the beam and adjusted the BPMs attenuation to 0 again;
- We disabled the orbit interlock and injected 10 mA spread over all bunches;
- We reacquired the sum thresholds and re-enabled the orbit interlock;
- We finished the injection up to 100 mA and left the beam with all loops closed and in top-up mode;

This experiment confirmed that the element that is heating is the bellows between the vertical scraper and the dipole kicker, because the other sensors farther from the bellows heated less. During the experiment we recovered the information that there are four bellows in the injection straight that are different than all others. They have an elliptical cross section, instead of a round one. The bellows with this characteristic are:

- The one at the entrance of the vertical scraper. This bellows is associated with temperature sensor MD3;

- The one ate the exit of the vertical scraper, associated with the sensor MD4. This is the one that is heating the most;
- Between the dipole kicker and the non-linear kicker, associated with MD5. This one also heated, but less than the previous one;
- At the exit of the non-linear kicker, associated with ED1. It also didn't heat.

This is an indication that this specific bellows must have some mechanical peculiarity in relation to the other 3 bellows. On the other hand, since none of the round bellows of the machine heated, the impedance of this type of elliptical bellows must be more sensitive to mechanical variations.

References

[1] Wikipedia contributors. *Discrete Fourier transform — Wikipedia, The Free Encyclopedia*. https://en.wikipedia.org/w/index.php?title=Discrete_Fourier_transform&oldid=1153873152. [Online; accessed 24-July-2023]. 2023.